Click Here for Full Article

Analysis of a potential "solar radiation dose–dimethylsulfide–cloud condensation nuclei" link from globally mapped seasonal correlations

S. M. Vallina,[1,2] R. Simó,[1] S. Gassó,[3] C. de Boyer-Montégut,[4,5] E. del Río,[1] E. Jurado,[6] and J. Dachs[6]

[1]   The CLAW postulate states that an increase in solar irradiance or in the heat flux to the ocean can trigger a biogeochemical response to counteract the associated increase in temperature and available sunlight. This natural (negative) feedback mechanism would be based on a multistep response: first, an increase in seawater dimethylsulfide concentrations (DMS_w) and therefore its fluxes to the atmosphere (DMS_{flux}); second, an increase in the atmospheric cloud condensation nuclei (CCN) burden as a consequence of DMS oxidation to form biogenic CCN (CCN_{bio}); and third, an increase in cloud albedo due to higher CCN numbers. Monthly global climatological fields of the solar radiation dose in the upper mixed layer (SRD), surface oceanic DMS_w, model outputs of hydroxyl radical concentrations (OH), and satellite-derived CCN numbers (CCN_s) are analyzed in order to evaluate the proposed "solar radiation dose-DMS-CCN" link from a global point of view. OH is included as the main atmospheric oxidant of the estimated DMS_{flux} to produce CCN_{bio}. Global maps of seasonal correlations between the variables show that the solar radiation dose is highly (positively) correlated with seawater dimethylsulfide over most of the global ocean and that atmospheric DMS oxidation is highly (positively) correlated with CCN_s over large regions. These couplings are stronger at high latitudes, whereas the regions with negative or no correlation are located at low latitudes around the equator. However, CCN_{bio} estimates for 15 regions of the global ocean show that DMS oxidation can be an important contributor to the CCN_s burden only over pollution-free regions, while it would have a minor contribution over regions with high loads of continental aerosols. Globally, the mean annual contribution of CCN_{bio} to total CCN_s is estimated to be $\approx 30\%$. Our results support that an oceanic biogenic mechanism that modulates cloud formation and albedo can indeed occur, although its impact seems rather weak over regions under a strong influence of continental aerosols. Nevertheless, our approach does not fully rule out that the observed correlations are due to an independent seasonal variation of the studied variables; seasonal couplings are necessary but not sufficient conditions to prove the CLAW hypothesis.

1. Introduction

[2]   One of the most important questions regarding Earth system functioning is if the biota in the global ocean respond to climate variations in ways that in turn impact climate conditions, thereby setting natural modulating mechanisms [e.g., *Charlson et al.*, 1987; *Miller et al.*,

[1]Institut de Ciències del Mar de Barcelona–Consejo Superior de Investigaciones Científicas (ICM–CSIC), Barcelona, Spain.

[2]Now at Laboratory for Global Marine and Atmospheric Chemistry, School of Environmental Sciences, University of East Anglia, Norwich, UK.

[3]Goddard Earth Science and Technology Center, University of Maryland, Baltimore County, Baltimore, Maryland, USA.

[4]Laboratoire d'0céanographie Dynamique et de Climatologie (LODYC–UPMC), Paris, France.

[5]Now at Yokohama Institute for Earth Sciences, JAMSTEC-FRCGC, Yokohama, Japan.

[6]Institut d'Investigacions Químiques i Ambientals de Barcelona–Consejo Superior de Investigaciones Científicas (IIQAB–CSIC), Barcelona, Spain.

2003; *Sarmiento et al.*, 2004]. Despite much research effort having been invested, this issue is still not fully resolved. Many mechanisms have been proposed and among them the hypothesis that the marine biota could act to modulate climate through the emission of volatile sulfur and its impact on aerosols and cloud albedo [*Charlson et al.*, 1987] has received considerable attention. The oceans are the largest source of natural sulfur emissions to the atmosphere in the form of biogenic dimethylsulfide (DMS) [*Simó*, 2001]. Seawater DMS (DMS_w) follows a complex cycle where several types of organisms and chemical reactions are involved. Phytoplankton produce intracellular dimethylsulfoniopropionate (DMSP), the biochemical precursor of DMS, through enzymatic cleavage with involvement of the whole planktonic food web [*Simó*, 2001]. Recent works have pointed out that, although the DMS_w dynamics result from a web of biological and biogeochemical processes, they are driven mainly by physical variables [*Simó and Dachs*, 2002; *Toole and Siegel*, 2004; *Vallina and Simó*, 2007]. For example, from a global point of view, the depth of the upper mixed layer (UML) is the only variable needed to efficiently estimate DMS_w surface fields over ≈85% of the ocean's surface [*Simó and Dachs*, 2002]. Also, in the Sargasso Sea the amount of UV radiation received in the UML explains almost 80% of the DMS_w seasonal variability [*Toole and Siegel*, 2004].

[3] DMS is emitted to the atmosphere with a ventilation rate that depends on DMS_w concentration as well as on seawater temperature and wind speed [*Nightingale et al.*, 2000]. Once in the atmosphere DMS (DMS_a) undergoes a sequence of oxidative reactions through interaction mainly with the hydroxyl radical (OH) [*Savoie et al.*, 1989; *Chin et al.*, 2000; *Barrie et al.*, 2001; *Kloster et al.*, 2006], giving rise to a range of products. Among them, non-sea-salt sulfate (nss-SO_4) and, to a lesser extent, methanesulfonate (MSA) are of particular interest because of their potential to form cloud condensation nuclei (CCN) [*Cox*, 1997]. MSA and nss-SO_4 particles are highly hygroscopic and usually occur in the submicron size fraction [*Ayers et al.*, 1997; *Andreae et al.*, 1999; *Jourdain and Legrand*, 2001]. On these grounds, DMS emissions are thought to be the main source of CCN in the marine troposphere remote from land [*Liss et al.*, 1997].

[4] CCN are believed to have a prominent role in the Earth energetic balance through both the direct scatter of solar incident radiation as well as their influence on cloud albedo and lifetime [*Twomey*, 1974; *Albrecht*, 1989; *Kaufman et al.*, 2002]. The CLAW hypothesis [*Charlson et al.*, 1987] proposed that an increase in solar irradiance and/or Earth temperature could be at the origin of an increase of DMS_w and its fluxes to the atmosphere. This would imply an increase in nss-SO_4 and, therefore, in the atmospheric CCN burden, which in turn would increase cloud albedo (Twomey or first indirect effect) and lifetime (Albrecht or second indirect effect) then reducing the solar incident radiation and thus Earth temperature. However, recent global analyses suggest that sea surface temperature is not the driving mechanism of DMS dynamics but rather the solar radiation dose [*Vallina and Simó*, 2007]. If it can be shown that the main mechanisms and forces proposed to conform the CLAW hypothesis (DMS emission, DMS oxidation efficiency, CCN formation, solar radiation) vary seasonally, should they be in phase the hypothetical feedback would be more feasible and more efficient. If no seasonal couplings were observed between some or all of these key factors, then the feedback would be hardly observable and even hardly feasible. This is because DMS, unlike CO_2, is a short-lived gas that does not accumulate in the atmosphere. That is, seasonal couplings are a "necessary but not sufficient" condition for the CLAW hypothesis [*Bates et al.*, 1987]. However, in present Earth conditions, the dominant sources of nss-SO_4 on a global scale are anthropogenic [*Lefohn et al.*, 1999; *Smith et al.*, 2001]. Also, sea salt (SS) is a dominant contributor to total aerosol mass over much of the oceans [*Heintzenberg et al.*, 2000]. Both anthropogenic SO_4 and the small fraction of SS can be effective CCN precursors [*Van Dingenen et al.*, 1995; *Murphy et al.*, 1998; *Andreae et al.*, 2003]. Other potential sources of CCN are products from biomass burning [*Ross et al.*, 2003] and maybe small dust particles [*Arimoto*, 2001], both very abundant in large regions of the globe [*Ginoux et al.*, 2001]. Therefore, if a solar irradiance-DMS-CCN link exists, it should be more easily observable in oceanic regions where continental sources contribute little to aerosol seasonality.

[5] Coincidence between the seasonalities of the solar radiation dose and DMS_w has been observed at a subtropical oligotrophic ocean site [*Toole and Siegel*, 2004] as well as at a coastal site in the NW Mediterranean Sea [*Vallina and Simó*, 2007], a feature that can be partly explained through an antioxidant function for the DMSP/DMS system in phytoplankton cells [*Sunda et al.*, 2002]. Also, several authors have found seasonal couplings between DMS and CCN both at local and regional scales, mainly in unpolluted regions [*Andreae et al.*, 1999; *Ayers et al.*, 1997]. However, because of the geographic sparseness of sampling stations, there is a lack of studies addressing the issue from a global point of view. Optical sensors on satellites (e.g., MODIS) offer the possibility of making quasisynoptic measurements of atmospheric variables at a global scale, which allows the investigation of couplings between the marine biogenic sulfur emissions and the atmospheric aerosols at spatial-temporal scales relevant for potential climate regulation. As far as we know, the only previous work based on global satellite data to investigate the coupling between ocean microbiota and atmospheric aerosols is that of *Cropp et al.* [2005]. Both the CLAW hypothesis as well as the Iron hypothesis [*Martin et al.*, 1994] were invoked to explain the observed positive correlations. They considered the Aerosol Optical Depth (AOD) as a surrogate of both dust particles and/or nss-SO_4 particles from DMS oxidation. Dust carries iron that, through deposition, has the potential to fertilize large regions of the oceans where productivity is limited by the supply of this micronutrient. Iron fertilization could in turn impact DMS production and therefore atmospheric nss-SO_4 formation. This combined approach hampered the assessment of the influence of DMS alone on aerosols [*Cropp et al.*, 2005]. The present work is based on a similar methodology to look at seasonal couplings but we fully focus on two of the central postulates of the CLAW

hypothesis: first, if an increase (decrease) in solar irradiance could produce an increase (decrease) of DMS_w over the global ocean; and second, if any increase (decrease) of DMS_w can be linked to a CCN increase (decrease). We also evaluate the couplings between DMS and the fine mode aerosols since nss-SO_4 mainly belongs to this size fraction. Finally, the contribution of estimated biogenic CCN (CCN_{bio}) to total CCN numbers is evaluated region by region of the globe.

2. Data and Methodology

[6] Since we are interested in seasonal couplings, we base all the analyses on global monthly mean climatological data for the selected variables, with a $1° \times 1°$ spatial resolution.

2.1. Solar Radiation Dose and DMS Data

[7] Monthly global maps of daily averaged solar radiation dose in the UML (or SRD; $W\ m^{-2}$) are estimated assuming an exponential decay of the daily averaged surface solar irradiance (I_0) with depth (z),

$$SRD = I_{uml} = \frac{1}{MLD} \int_0^{MLD} I_0 * exp(-k * z)dz. \quad (1)$$

I_0 is assumed to be 50% of the daily averaged solar irradiance at the top of the atmosphere (I_{toa}; $W\ m^{-2}$) [Kiehl and Trenberth, 1997], which is calculated following Brock [1981]. The depths of the UML (MLD) are based on the work of de Boyer-Montégut et al. [2004]. This is the latest and most complete climatology of global MLD, based on more than 4,000,000 temperature profiles (from 1941 to 2002). We have made use of this climatology with a modification of the definition criterion: the depth of the mixed layer is calculated as the depth at which temperature departs $0.1°C$ from that at 5 m. We assume a general solar-radiation extinction coefficient (k) of 0.06 m^{-1}, which is a reasonable approximation for spectrum-centered wavelengths in open ocean waters [Smith and Baker, 1979; Kieber et al., 1996; Lee et al., 2005].

[8] The DMS_w global monthly fields are those of Kettle and Andreae [2000], which are based on the Global Surface Seawater DMS database, the biggest and most comprehensive compilation of DMS_w measurements available at that time (about 20,000 data points). This database was used to construct a global climatology of monthly means based on interpolation/extrapolation procedure to fill the large areas/seasons where no data were available [Kettle and Andreae, 2000]. DMS emissions to the atmosphere (DMS_{flux}) are calculated as a function of surface wind speed and sea water temperature (SST) using the gas transfer model of Nightingale et al. [2000]. Surface wind speed and SST data were obtained from the NOAA-CIRES Climate Diagnostics Center. Wind speed are model outputs, from the NCEP/NCAR Reanalysis project, constrained by contemporary data obtained from the SSM/I sensor (DMSP, NOAA) [Kistler et al., 2001]. SST is a climatology (1971–2000) based on field and satellite measurements [Reynolds and Smith, 1995].

2.2. Atmospheric Data

[9] The MODerate resolution Imaging Spectro-radiometer (MODIS), on board the Earth Observing System (EOS), currently has two detectors in orbit (on the satellites Terra and Aqua). Both have daily global coverage with a morning and afternoon pass respectively. In this study, we use data measured by MODIS-Terra. MODIS aerosol data ($1° \times 1°$ resolution) are available from NASA's Goddard Space Flight Center (GSFC) Distributed Active Archive Centers (DAAC). MODIS acquires data globally at 36 spectral bands (from 0.4 to 14.5 μm) and it is the first satellite capable of distinguishing coarse and fine aerosols, especially over the ocean [Ichoku et al., 2004]. Several primary aerosol parameters are retrieved from MODIS daytime data over the ocean, including the fine mode fraction or ETA (η) parameter [Remer et al., 2005]. Ranging from 0 to 1, ETA is defined as the ratio of the AOD contributed by the small mode particles (or accumulation mode) to the total AOD (AOD_{small}/AOD_{total}) and can thus be viewed as a measure of the percentage of fine particles that contribute to the total aerosol burden. SS and dust are mainly composed of coarse particles while nss-SO_4 belongs to the accumulation mode [Fitzgerald, 1991; Andreae et al., 1999; Jourdain and Legrand, 2001]. If DMS contributes significantly to the aerosol burden, the ETA parameter should be higher in regions and seasons with higher DMS oxidation. On the other hand, regions dominated by SS or dust inputs should display low ETA values.

[10] From the primary parameters retrieved by MODIS, it is possible to derive secondary products such as column-integrated CCN numbers (in units of partic cm^{-2}) [Tanré et al., 1999; Gassó and Hegg, 2003]. In the present work, CCN concentrations are obtained with the derivation method described by Gassó and Hegg [2003]. The method, which is based on atmospheric optical properties, derives the maximum number of particles in the accumulation mode and provides an upper end estimate of the concentration of particles that may act as CCN at $\approx$0.2% supersaturation. We call this satellite-based CCN estimates as CCN_s. The method allows for the adjustment of coefficients according to the type of aerosols that are present. Because we are interested in marine aerosols, the CCN_s algorithm coefficients (the aerosol refraction index and the aerosol density) were adjusted to be representative of the main aerosol types present in marine regions: SS, nss-SO_4 and MSA.

[11] Global OH concentrations in the marine boundary layer (MBL) are outputs of the GEOS-CHEM model run by the Atmospheric Chemistry Modeling Group at Harvard University [Fiore et al., 2003]. GEOS-CHEM simulates atmospheric composition using assimilated meteorological observations from the Goddard Earth Observing System (GEOS) of the NASA Global Modeling and Assimilation Office. Monthly OH distributions are available only for 2001.

[12] Atmospheric MSA monthly climatologies for several locations all around the globe were obtained from the measurements of the University of Miami network of aerosol sampling stations (12 locations) [Chin et al., 2000], the Australian Baseline Air Pollution Station [Ayers and Gillett, 2000] (Cape Grim), as well as the measurements of Sciare et

al. [1998] (Amsterdam Island) and *Kubilay et al.* [2002] (Crete). All data correspond to aerosol-associated MSA except for Amsterdam Island, where only MSA concentrations in rainwater (for 1996) are available.

2.3. DMS Oxidation

[13] OH is the main oxidant of DMS_a to produce MSA and nss-SO_4 through a series of reactions that occur during daytime [*Kloster et al.* 2006]. Therefore the amount of potential biogenic CCN depends not only on the DMS_{flux} but also on OH concentrations. Higher amount of OH respect to the amount of DMS_{flux} would imply a higher DMS oxidation efficiency [*Gondwe et al.*, 2004]. The resulting potential biogenic CCN can be characterized as follows:

$$CCN_{bio} = b * \gamma * DMS_{flux}, \qquad (2)$$

where b is a unit conversion constant and γ is a dimensionless parameter varying between 0 a 1 that gives the efficiency of DMS oxidation as function of the ratio between OH and DMS_{flux} following an equation of the form

$$\gamma = \frac{x}{k_s + x}, \qquad (3)$$

where $x = \frac{OH}{DMS_{flux}}$. In the absence of OH (or very low OH) concentrations respect to the DMS_{flux}, most (or at least part) of the DMS_{flux} cannot be converted to CCN_{bio} (in this situations γ will be low). On the other hand, if OH concentrations are in excess all the DMS_{flux} can be oxidized to CCN_{bio} (in this situations γ will be close to one). The form of the equation accounts for an asymptotic behavior; as the availability of OH for DMS oxidation (the variable x) increases, a higher fraction of the DMS_{flux} can be converted to CCN_{bio} approaching asymptotically the upper limit of gamma (for which all DMS_{flux} is converted to CCN_{bio}). Therefore γDMS_{flux} gives the amount of biogenic sulfur potentially available for CCN production. The constant (k_s) corresponds to the value of x that gives a γ of 0.5 (a DMS oxidation efficiency of 50%). Assuming an annual-averaged DMS oxidation efficiency for the Southern Ocean (SO, defined as the area comprised between 40°S and 60°S) of 50% [*Shon et al.*, 2001], we obtained a value of k_s from the annual averages of OH, DMS_{flux} over the SO. In order to evaluate the potentiality of DMS oxidation as a source of biogenic aerosols, we will compare the seasonal evolution of the estimated atmospheric DMS oxidation (γDMS_{flux}) against the seasonality of MSA (an exclusive product of DMS oxidation) in aerosols from 15 sampling stations of the world cited above. The monthly γDMS_{flux} series that are compared with station-based MSA series come from averaging the 49 points taken by placing a 7° × 7° window upwind of each station.

2.4. Globally Mapped Seasonal Correlations

[14] Three years of surface wind speed, CCN_s and ETA monthly means (from January 2002 to December 2004) were combined to create a 1-year climatology for each variable. These are used to evaluate the seasonal couplings between variables of interest: SRD versus DMS_w, DMS_{flux} versus OH, γDMS_{flux} versus CCN_s and ETA. The global maps of seasonal correlations are based on the following procedure: using a running window of 7° × 7°, we obtained for each position (latitude, longitude) of the global ocean (i.e., for every 1° × 1° grid box) time series of 12 points (months) for the pair of variables we want to analyze. Each of the 12 points of the time series is the average of the 49 values taken by the running window in a given month. Then, for every 1° × 1° grid box of the global ocean we calculate the seasonal (Spearman) correlation coefficient between the two variables (12 degrees of freedom), generating a global map of seasonal correlations (significant correlations at 95% confidence level for $|r| > 0.5$ and at 80% confidence level for $|r| > 0.4$). Prior to the global analysis all fields are smoothed with a 3° latitude × 3° longitude × 3 months running mean [*Wilson and Coles*, 2005].

3. Results and Discussion

3.1. Global Maps of Seasonal Correlations

[15] Figure 1a shows that there is a strong seasonal coupling between the solar radiation dose in the UML and oceanic DMS_w concentrations, in agreement with the first postulate of the CLAW hypothesis that we are evaluating. Further, this coupling seems to be present almost everywhere in the global ocean. The areas where there is negative or no correlation are located mostly in the equatorial region. Owing to the very low seasonality of these latitudes, any error or uncertainty in the monthly DMS_w fields can generate a noise with higher amplitude than the underlying seasonality, thus largely affecting the correlation coefficient. These results are in agreement with recent works that have identified light as being the driving force of DMS in oligotrophic waters of the Sargasso Sea [*Toole and Siegel*, 2004] and NW Mediterranean [*Vallina and Simó*, 2007]. Long-term measurements conducted in several locations of the world have also shown that DMS generally increases in summer [*Berresheim et al.*, 1991; *Ayers et al.*, 1997; *Ayers and Gillett*, 2000; *Sciare et al.*, 2000; *Jourdain and Legrand*, 2001; *Kouvarakis and Mihalopoulos*, 2002; *Toole and Siegel*, 2004; *Vallina and Simó*, 2007].

[16] Owing to the role of the OH radical as the main DMS oxidizer to nss-SO_4 and MSA, any coupling or mismatch between the seasonalities of OH and the DMS_{flux} will amplify or buffer the seasonal contribution of biogenic sulfur to CCN production. The seasonal coupling between DMS_{flux} and OH radical is very strong over most parts of the globe (see Figure 1b). Therefore summer months are characterized by both higher DMS emission and a better efficiency in the oxidation of DMS into CCN, that is, higher potential to counteract higher solar irradiances.

[17] Figure 2 displays the seasonal couplings between γDMS_{flux} and MSA for 15 locations of the globe. In general we observe an excellent seasonal agreement between the two variables. Therefore our DMS oxidation proxy is able to capture MSA seasonality, as it should be if DMS oxidation is fuelling MSA production. A quantitative vali-
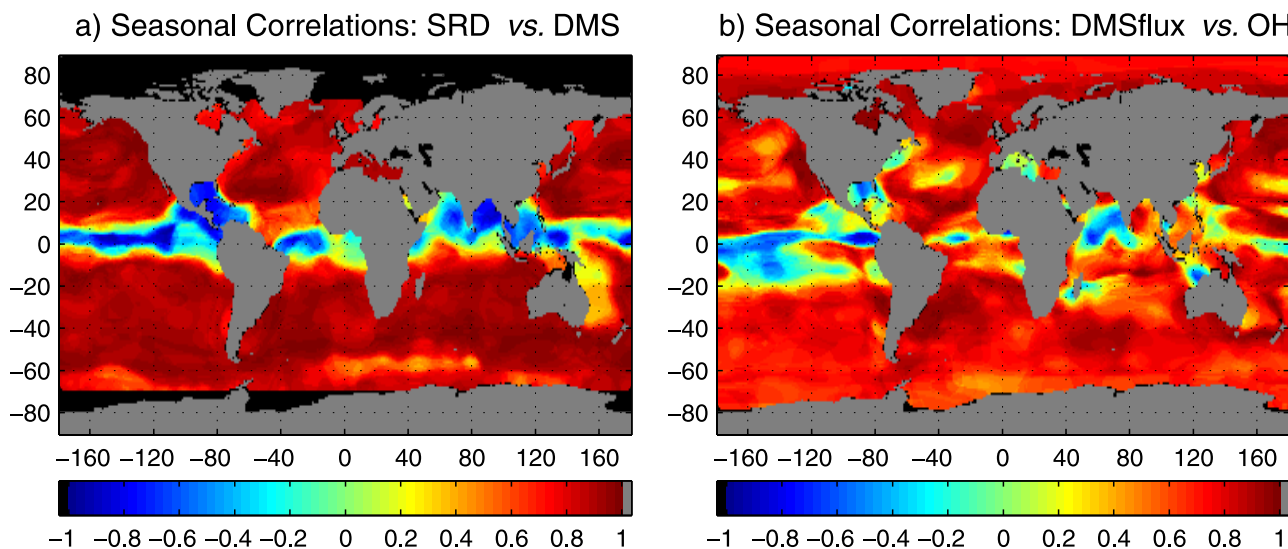
Figure 1. Global map of seasonal correlations between: (a) the solar radiation dose in the upper mixed layer and climatological monthly aqueous DMS concentrations (from *Kettle and Andreae* [2000]), and (b) the estimated DMS flux to the atmosphere [from *Nightingale et al.* 2000] and monthly hydroxyl-radical atmospheric concentrations [from *Fiore et al.*, 2003].

dation with MSA is not appropriate since the biogenic nss-SO_4 to MSA ratio from the gas-phase DMS oxidation is very variable between regions (up to a factor of 6) because it is temperature dependent, being much lower at high latitudes [*Savoie et al.*, 2002]. At Stations 5 and 13 the correlation coefficients between DMS oxidation and MSA are not significant. Station 5 is located in Japan (NE Pacific), a region subject to high levels of polluted aerosols in spring [*Husar et al.*, 1997; *Tanré et al.*, 2001; *Prospero et al.*, 2003]. Therefore the observed spring peak of MSA could be related to an heterogeneous nucleation of MSA on polluted aerosols. While DMS_a concentration in polluted air is generally much lower than in oceanic air masses, MSA concentrations are usually found to be also high in polluted air masses [*Berresheim et al.*, 1991; *Wylie and de Mora*, 1996], which may reflect its adsorption on preexisting continental aerosols. On the other hand, Station 13 (American Samoa, $14.25°S–170.5°W$) is a very clean oceanic region almost free from continental influences [*Savoie et al.*, 1989, 1994]. The low seasonality of this tropical location is probably the cause of the nonsignificant correlation. Similar results are obtained using MSA data from Fanning Island (not shown), located near the equator ($3.85°N–159.36°W$). At these two locations, MSA data does not show a clear seasonal cycle [*Savoie and Prospero*, 1989; *Savoie et al.*, 1994].

[18] Figures 3a and 3b show the seasonal couplings between DMS oxidation against CCN_s and ETA respectively, where it can be observed that large regions of the global ocean display strong positive correlations. This is especially true, as expected, at high latitudes, where the seasonal amplitude of DMS_w is higher. Of special interest is the SO ($40°S–60°S$) since it is a remote region weakly impacted by continental aerosols [*Quinn et al.*, 1998; *Andreae et al.*, 1999; *Ayers and Gillett*, 2000; *Prospero et al.*, 2002] where DMS_a concentrations are very high in austral spring and

summer [*Curran and Jones*, 1998]. For example, at Cape Grim DMS_a displays a strong seasonality [*Ayers et al.*, 1995]. Further, summertime SO_2 concentrations in this pristine region are predominantly of marine origin [*De Bruyn et al.*, 1998]. During austral summer, a band of relatively high CCN_s concentrations is clearly observed over the SO (see DJF plot in Figure 4). This CCN_s band does not display spatial gradients coming from continents, which is a strong indication of a marine origin. SS does not seem either to be the source of this austral summer high aerosol band [*Husar et al.*, 1997; *Vallina et al.*, 2006]. Its DMS-related origin is supported by the seasonality of the fine mode aerosols (Figure 5) [see also *Vallina et al.*, 2006], field observations in the region [*Davison et al.*, 1996; *Andreae et al.*, 1999] as well as modeling works [*Yoon and Brimblecombe*, 2002; *Gondwe et al.* 2003; *Kloster et al.* 2006].

[19] Strong positive correlations between DMS oxidation and CCN_s (as well as ETA) are also found over oceans where nss-SO_4 inputs from anthropogenic sources are known to be higher than nss-SO_4 inputs from DMS (i.e., North Atlantic, North Pacific) [*Berresheim et al.*, 1981; *Van Dingenen et al.*, 1995; *Prospero*, 1996; *Nagao et al.*, 1999; *Chin et al.*, 2000; *Andreae et al.*, 2003]. This can be also observed through much higher CCN_s numbers present in these regions during the boreal summer (JJA) compared to CCN_s numbers over the SO during the austral summer (Figure 4). It is obvious that there is a general trend toward higher aerosol numbers in each hemispheric summer [*Husar et al.*, 1997] (Figure 4). While to some extent this fact can be related to atmospheric circulation changes (e.g., the increase of aerosol loading during the boreal summer in the Caribbean Sea is due to a northern shift, following the ITCZ movement, of the dust pathway coming from Africa [*Prospero*, 1996; *Perry et al.*, 1997; *Ginoux et al.*, 2001]) or precipitation seasonality (e.g., biomass burning usually
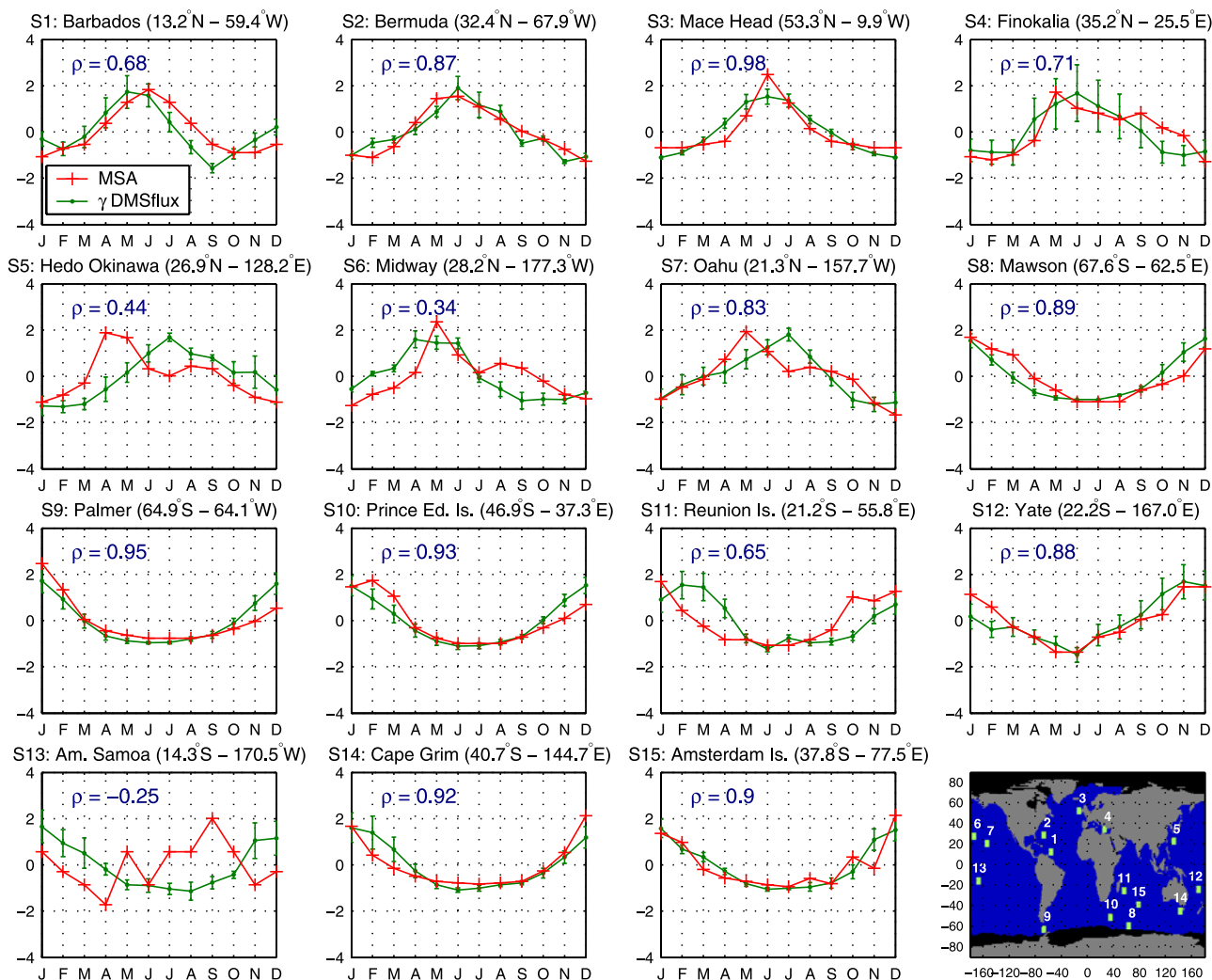
Figure 2. Seasonal evolution and the associated Spearman correlation coefficient of the atmospheric DMS oxidation against monthly climatological methanesulfonate concentrations in aerosols at 15 locations of the globe. (Variables are presented in standardized form, i.e., subtracting the mean and dividing by the standard deviation).

increases during the dry season peaking in each hemispheric spring [*Duncan et al.*, 2003]), in some regions it is certainly related to the oxidation of SO_2 to form nss-SO_4 aerosols [*Rasch et al.*, 2000; *Chin et al.*, 2000; *Barrie et al.*, 2001]. For example, in the North Atlantic, which is heavily impacted by pollution from Europe and North America [*Van Dingenen et al.*, 1995; *Husar et al.*, 1997; *Andreae et al.*, 2003], the levels of nss-SO_4 clearly increase in boreal summer, despite anthropogenic SO_2 emissions in these regions being fairly constant throughout the year [*Smith et al.*, 2001; *Andreae et al.*, 2003] (or even slightly higher in boreal winter in Europe [*Chin et al.*, 2000; *Rasch et al.*, 2000; *Smith et al.*, 2001; *Rotstayn and Lohmann*, 2002]) and SO_2 concentrations display a summer minimum due to the higher oxidative efficiency to form nss-SO_4 [*Berresheim et al.*, 1991; *Chin et al.*, 2000; *Rasch et al.*, 2000; *Rotstayn and Lohmann*, 2002]. The summertime increase of nss-SO_4 and CCN_s in the North Atlantic is therefore not related to the seasonality of their precursor SO_2 but to its increased oxidation efficiency by OH. On the other hand, in relatively pollution-free regions like Amsterdam Island (37.8°S–77.5°E) the SO_2 increase in summer is probably due to a DMS origin [*Rotstayn and Lohmann*, 2002; *Kloster et al.*, 2006]. We must conclude, therefore, that atmospheric oxidation efficiencies are an important actor in aerosol production. This supports that SO_2 (whatever its origin, anthropogenic or DMS) is indeed able to fuel new particle formation and it is responsible for a nonnegligible fraction of the observed CCN_s.

[20] The areas with low or negative correlations between DMS oxidation and CCN_s or ETA are mostly in the equatorial to tropical regions (Figure 3). These are latitudes where the DMS concentration and flux show low seasonal variability, which precludes from finding significant correlations using a seasonal correlation analysis. Moreover, these are regions with high loads of continental aerosols (mostly dust and biomass burning particles) that can also contribute to satellite-retrieved CCN_s numbers (Figure 4).
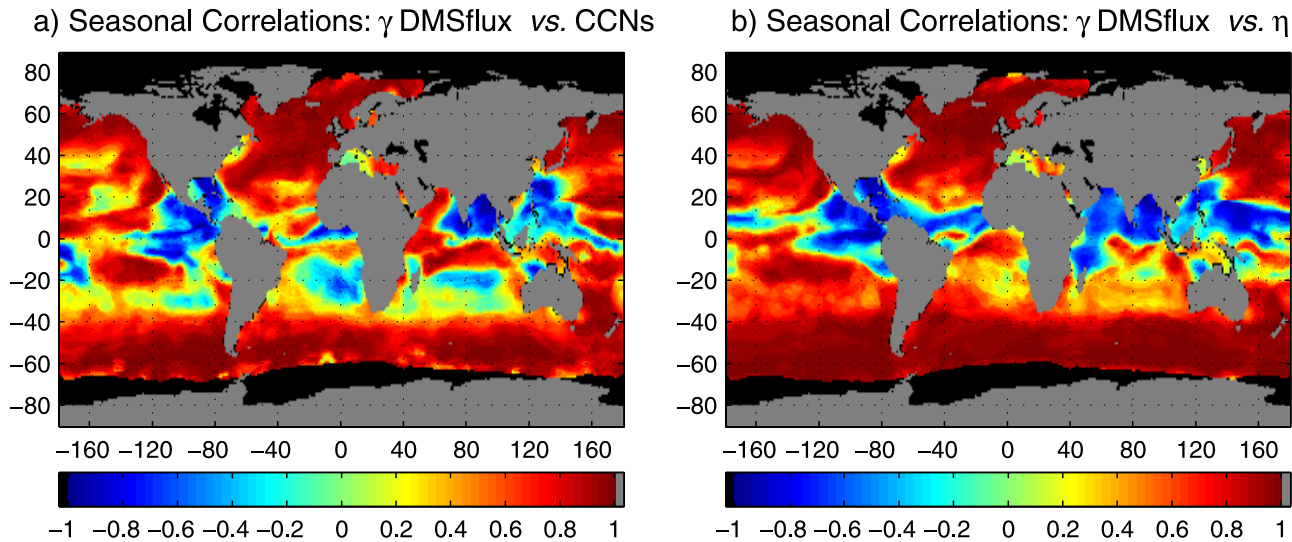
Figure 3. Global map of seasonal correlations between atmospheric DMS oxidation and: (a) monthly climatological (years 2002 to 2004) satellite-derived CCN concentrations (using the method of *Gassó and Hegg* [2003]), (b) monthly climatological (years 2002 to 2004) satellite-derived contribution of small mode particles to the Aerosol Optical Depth (ETA parameter = AOD_{small}/AOD_{total}) as provided by MODIS.

For example, the very high values of CCN_s observed off the tropical West Africa (see Figure 4) are strongly contributed by aerosols from biomass burning [*Husar et al.*, 1997; *Tanré et al.*, 2001; *Kaufman et al.*, 2002; *Duncan et al.*, 2003]. This is also the case over the Pacific off Central America and the Indonesian region [*Husar et al.*, 1997; *Deuzé et al.*, 1999; *Tanré et al.*, 2001; *Duncan et al.*, 2003]. This can also be observed in Figure 5 since biomass burning aerosols are mostly accumulation mode particles (therefore the ETA parameter is very high). Interestingly, the Arabian Sea shows a positive correlation between DMS oxidation and CCN_s while it is negative between DMS oxidation and ETA. This is an indication that the observed increase of CCN_s in boreal summer in this region (see the JJA plot in Figure 4) is not related to an increase of small aerosols but to an increase of coarser aerosols, and therefore that they do not come from DMS oxidation. This is in agreement with previous works that have found an increase of both dust from the Arabian Peninsula (at high altitudes) along with an increase of SS concentrations (at low altitudes) due to the strong winds of the SW monsoon [*Husar et al.*, 1997; *Tindale and Pease*, 1999; *Li and Ramanathan*, 2002]. A similar situation is observed in the region between off Northwestern Africa (around 10°N) and northern South America, a well known path for African dust [*Swap et al.*, 1992]. Although dust and SS aerosols mainly belong to coarse particles, a fraction of them can be present in the accumulation mode [*Perry et al.*, 1997; *Murphy et al.*, 1998; *Satheesh et al.*, 1999], then affecting CCN_s retrieval. Therefore, in order to infer which regions could be under biogenic aerosol production it is necessary to combine the analysis of global correlation maps of DMS oxidation against CCN_s as well as against the ETA parameter. An

increase of biogenic CCN_s should be followed by an increase of ETA.

3.2. Biogenic Contribution to CCN Numbers

[21] The correlation analyses have shown that in large regions of the ocean the DMS oxidation and CCN_s are seasonally coupled, but this type of analysis does not provide any quantitative information about the contribution of biogenic CCN_s to total CCN_s numbers over the oceans. To obtain such information, we first focus on the SO since this is the region where CCN seasonality is believed to be driven mainly by DMS oxidation [*Ayers et al.*, 1997; *Husar et al.*, 1997; *Ayers and Gillett*, 2000; *Gondwe et al.*, 2003, 2004; *Kloster et al.*, 2006; *Vallina et al.*, 2006]. We calculate the spatial mean value of γDMS_{flux} and CCN_s for each month over the whole SO area between 40°S and 60°S (therefore obtaining 12 data points). A regression analysis γDMS_{flux} versus CCN_s is then applied in order to estimate the value of the slope b of equation (2) for this region. Results are shown in Figure 6. The determination coefficient is high ($r^2 = 0.83$) and close to the value of $r^2 = 0.84$ obtained by *Ayers et al.* [1997] using climatological DMS_a and CCN from in situ measurements at Cape Grim (40.7°S–144.7°E). Further, using the normalized data (values divided by its annual mean), we obtain similar (normalized) regression coefficients to those of *Ayers et al.* [1997]. The (normalized) intercept is 0.41 (it was 0.48 at Cape Grim) and the (normalized) slope is 0.59 (it was 0.52 at Cape Grim) (see the equation in brackets in Figure 6).

[22] If over the SO CCN numbers are linked to DMS oxidation, this link between biogenic CCN and DMS must occur also over other regions, yet it could be hidden by continental CCN sources over less pristine areas. Assuming that the slope value $b = 3.57$ obtained for the SO (Figure 6)
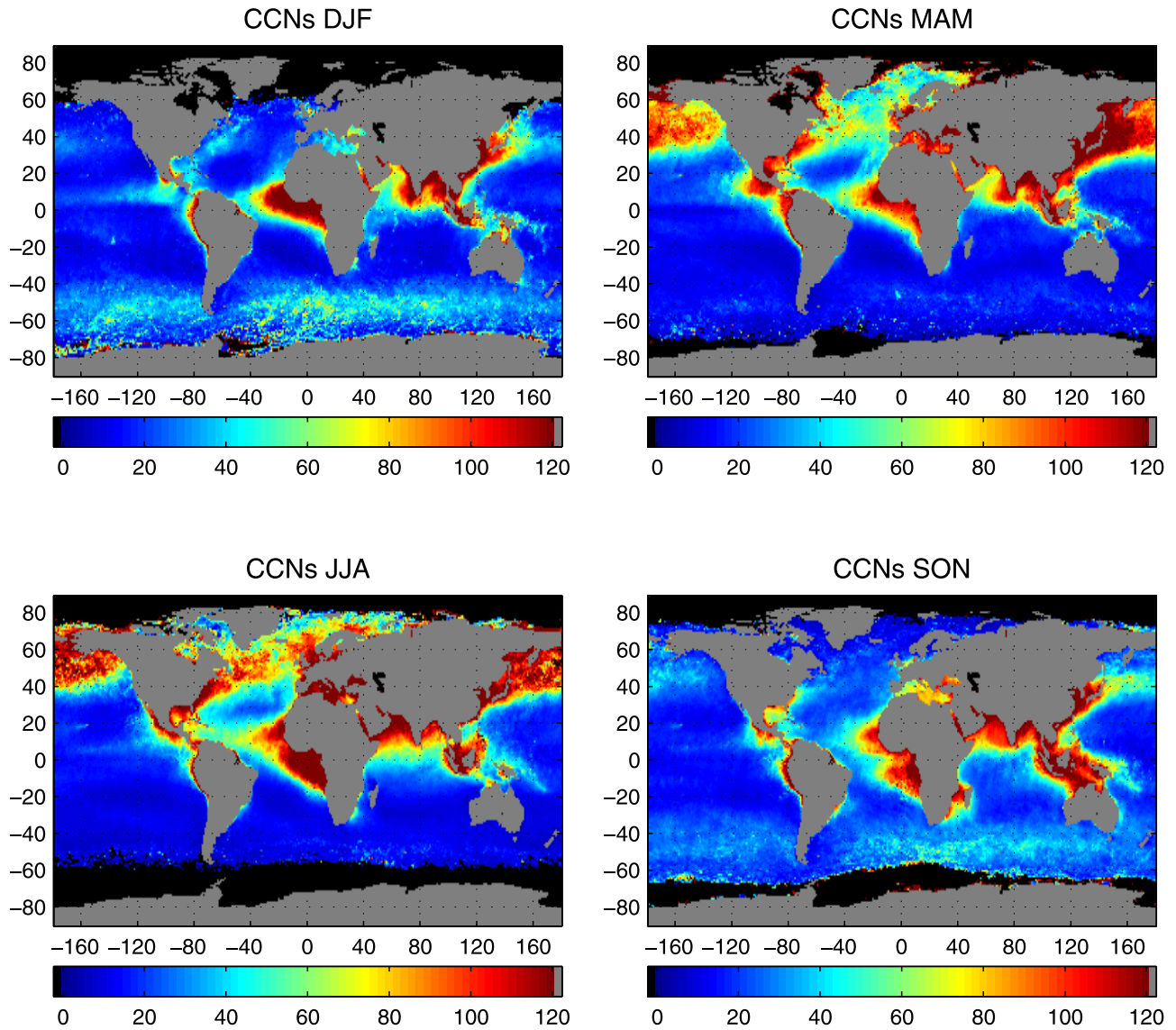
Figure 4. Global maps of monthly climatological (years 2002 to 2004) satellite-derived CCN concentrations (partic cm^{-2}; using the method of Gassó and Hegg [2003]) for the four seasons. DJF, December to February; MAM, March to May; JJA, June to August; SON, September to November.
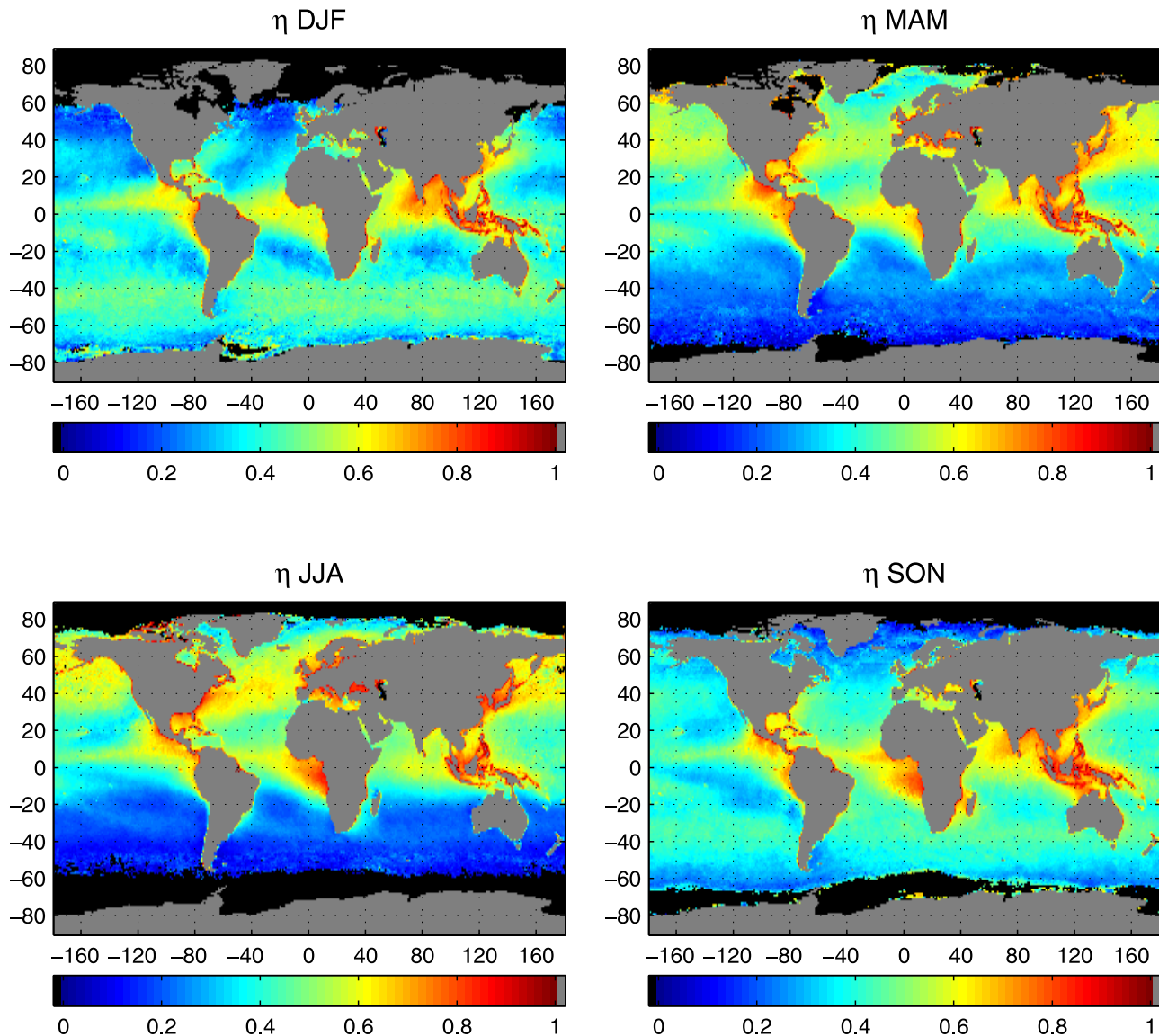
Figure 5. Global maps of monthly climatological (years 2002 to 2004) satellite-derived contribution of small mode particles to the Aerosol Optical Depth (ETA parameter = AOD_{small}/AOD_{total}) (as provided by MODIS) for the four seasons. DJF: December to February; MAM: March to May; JJA: June to August; SON: September to November.

is valid for other regions, we apply equation (2) in order to estimate CCN_{bio} from DMS oxidation fluxes in 15 regions of the global ocean (the value of the intercept, 9.29, is assumed to be a constant background of SS fine mode aerosols [*Andreae et al.*, 1999] and then it is subtracted to take into account only the biogenic contribution [*Vallina et al.*, 2006]). Nevertheless CCN formation is a very complex process that depends on many factors (such as aerosol composition, aerosol size and supersaturation). All these factors are certainly different for the regions in which we apply the regression derived for SO conditions. However, up to now all these processes are not well enough understood to include them into our analysis. Results are shown in Figure 7, where ρ is the (Spearman) correlation coefficient between CCN_{bio} and CCN_s, and $\beta = \dfrac{\sum CCN_{bio}}{\sum CCN_s} * 100$ is

the annual contribution of biogenic derived CCN_s to the total CCN_s.

[23] CCN_{bio} contributes annually about a 60% to the total CCN_s in the SO (region 14; from about 30% in austral winter to 80% in austral summer [see also *Vallina et al.*, 2006], being the remaining CCN_s probably small SS [*Andreae et al.*, 1999; *Vallina et al.*, 2006]. However, the estimated CCN_{bio} fraction for the Antarctic (region 15) is only 24%. The very low model OH concentrations present in this high-latitude region give rise to very low values of γ (<0.3 for all months except for October and November with ≈0.55), therefore reducing the estimated DMS available for CCN production. Nevertheless, in situ measurements of MSA and nss-SO_4 suggest that DMS plays a primary role in the atmospheric sulfur cycle over the Antarctic continent
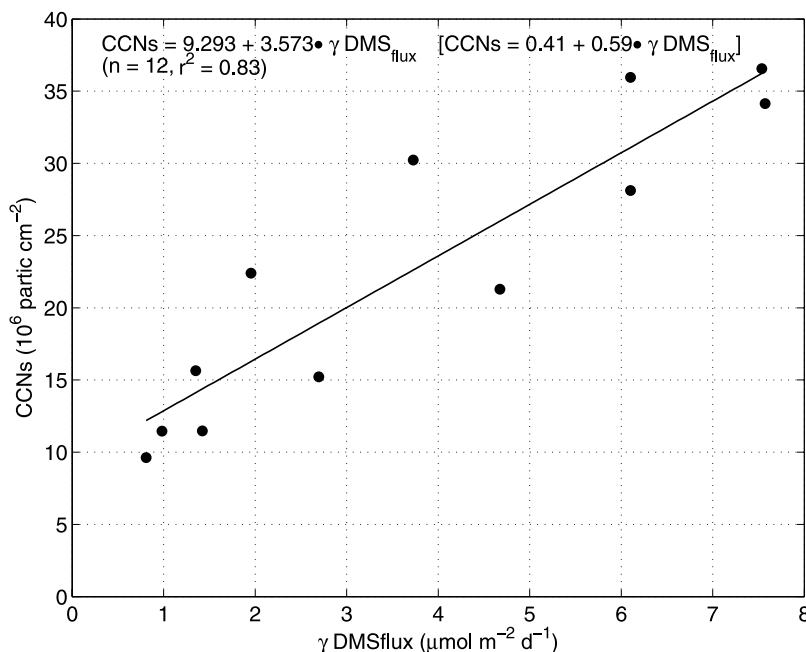
Figure 6. Regression analyses of atmospheric DMS oxidation against monthly climatological (years 2002 to 2004) satellite-derived CCN concentrations (using the method of *Gassó and Hegg* [2003]) for the Southern Ocean (defined as the area comprised between 40°S and 60°S).

[*Savoie et al.*, 1992; *Minikin et al.*, 1998]. Thus further research is needed in this region. It has been proposed that a large fraction of DMS_a is transported out of the marine boundary layer (MBL) where, in the presence of high OH and low aerosol scavenging, oxidized sulfur species accumulate and are entrained episodically back into the MBL [*Davis et al.*, 1998].

[24] Other regions where DMS oxidation could be a significant source of CCN are the subtropical Atlantic (both hemispheres; regions 2 and 4), and the subtropical South Pacific and Indian oceans (regions 8 and 12 respectively). In the subtropical North Atlantic (region 2), although there is a good correlation between CCN_{bio} and CCN_s ($\rho = 0.72$), the absolute contribution is rather moderate ($\beta = 38\%$). Only over the western part DMS may contribute up to 75% of the sulfur budget under easterly winds, although under westerly winds anthropogenic sulfur from North America dominates [*Berresheim et al.*, 1991]. Also, in boreal spring and summer this region is also under the influence of supra-micron particles of African dust plumes coated with SO_4 from Europe [*Li-Jones and Prospero*, 1998]. In April at Barbados (13.15°N–59.30°W), when dust and pollution levels are low, the dominant source of nss-SO_4 is ascribed to DMS and the submicron fraction dominates (up to 80%) [*Li-Jones and Prospero*, 1998]. Annually, the estimated DMS contribution to the nss-SO_4 at Barbados and Bermuda (32.27°N–64.87°W) is ≈50% and ≈30% respectively [*Savoie et al.*, 2002]. The subtropical South Atlantic (region 4, $\beta = 56\%$) displays a seasonal CCN_s maximum in September not related to CCN_{bio} but to biomass burning over tropical Africa [*Husar et al.*, 1997; *Deuzé et al.*, 1999; *Goloub and Arino*, 2000; *Tanré et al.*, 2001; *Duncan et al.*, 2003; *Ross et al.*, 2003] (see also SON plot in Figures 3 and 4). African biomass burning aerosols are also transported

over Madagascar and the subtropical Southern Indian Ocean (region 12, $\beta = 67\%$) in October, the burning season in Southeastern Africa [*Deuzé et al.*, 1999; *Goloub and Arino*, 2000; *Duncan et al.*, 2003] (see also SON plot in Figures 3 and 4). This explains why the obtained seasonal correlations are not significant for regions 4 and 12 ($\rho = -0.32$ and 0.31 respectively) while the biogenic contribution is significant. Over the subtropical South Pacific (region 8) CCN_{bio} are significantly correlated to CCN_s ($\rho = 0.68$) and the estimated biogenic contribution is very high ($\beta = 99\%$). This is in agreement with field studies which have found that marine-derived DMS may provide essentially all of nss-SO_4 over the tropical South Pacific [*Savoie et al.*, 1989].

[25] In many of the regions, however, it is clear that the estimated CCN_{bio} has a minor annual contribution to the total CCN_s. This is the case of the North Atlantic (region 1, $\beta = 29\%$), a region known for being under the influence of heavily polluted air masses from Europe and North America in spring and summer [*Van Dingenen et al.*, 1995; *Husar et al.*, 1997; *Andreae et al.*, 2003]. For example, at Mace Head (53.32°N–9.85°W) the annual biogenic contribution to nss-SO_4 is estimated to be less than 15% [*Savoie et al.*, 2002]. In boreal spring, DMS contribution to nss-SO_4 is also estimated in ≈10% [*Andreae et al.*, 2003]. Regarding CCN_s variability ($\rho = 0.92$), although CCN_{bio} in the North Atlantic are higher in summer, they can hardly account for the full CCN_s seasonality: if we subtract CCN_{bio} from total CCN_s, the remaining (putatively anthropogenic) CCN_s still have a summer-to-winter ratio of 2.25. Therefore higher summer-time oxidation of anthropogenic SO_2 is an important process affecting CCN seasonality over the North Atlantic.

[26] The equatorial Atlantic (region 3, $\beta = 11\%$) is highly impacted by biomass burning and dust from Africa, and the equatorial Indian Ocean (region 11, $\beta = 27\%$) by biomass
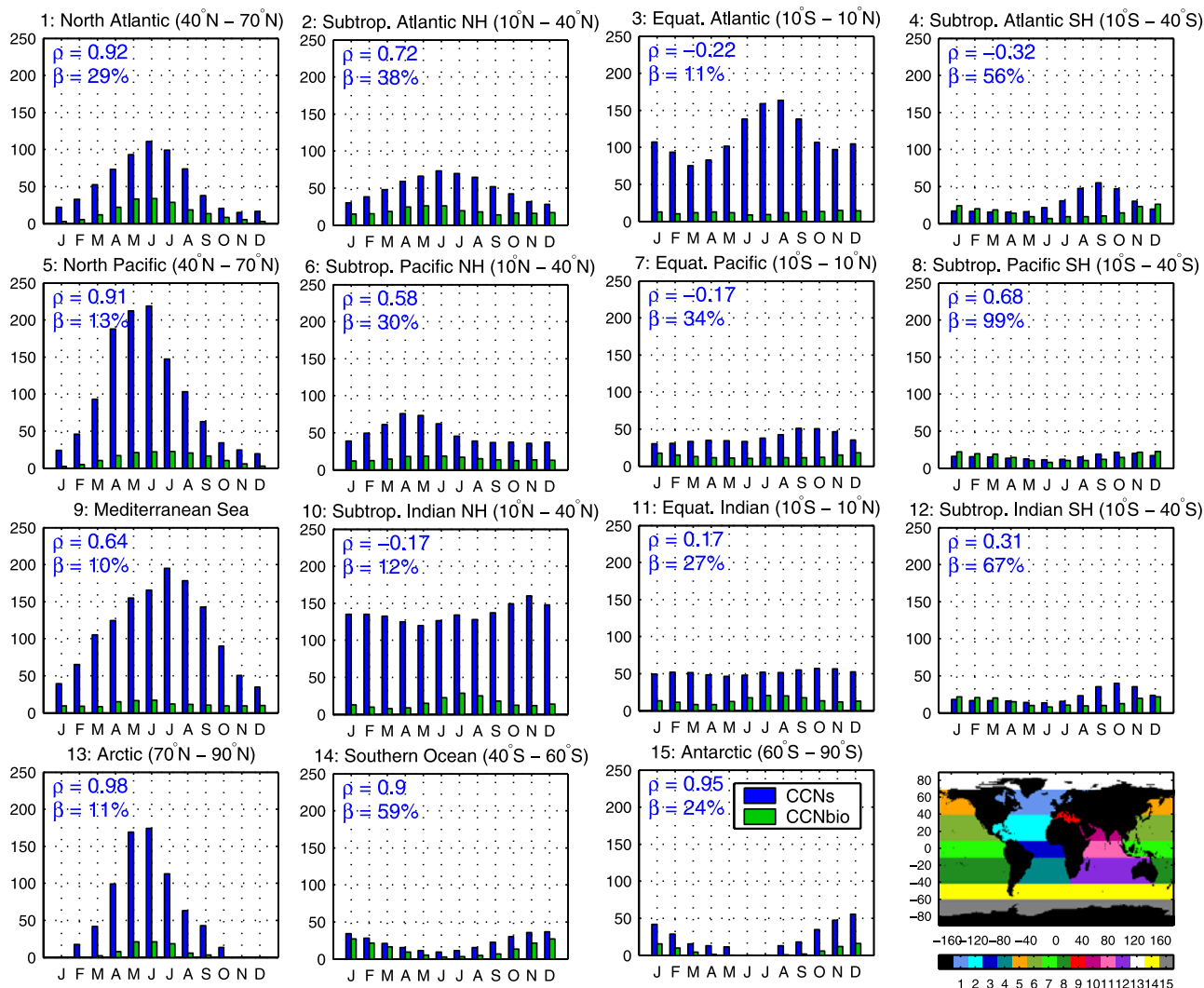
Figure 7. Seasonal evolution of monthly climatological (years 2002 to 2004) satellite-derived CCN concentrations (partic cm^{-2}; using the method of *Gassó and Hegg* [2003]) and the estimated biogenic CCN from DMS oxidation for 15 regions of the global ocean (ρ is the Spearman correlation coefficient between CCN$_{bio}$ and CCN$_s$, and $\beta = \frac{\sum CCN_{bio}}{\sum CCN_s} * 100$ is the annual contribution of CCN$_{bio}$ to the total CCN$_s$).

burning from the Indonesian region. In the equatorial Pacific (region 7), which is also impacted by biomass burning from Central America in spring [*Husar et al.*, 1997; *Deuzé et al.*, 1999; *Goloub and Arino*, 2000; *Tanré et al.*, 2001; *Kaufman et al.*, 2002; *Duncan et al.*, 2003], the estimated contribution of biogenic sulfur to CCN$_s$ numbers is a bit higher ($\beta = 34\%$). Nevertheless, in terms of sulfate aerosols, almost all nss-SO$_4$ over the equatorial Pacific (e.g., American Samoa, Fanning Island) has been suggested to originate from the oxidation of oceanic DMS [*Savoie and Prospero*, 1989; *Savoie et al.*, 1994]. Near the Christmas Islands (1.52°N–157.2°W), DMS has also been identified as the dominant source of MBL's SO$_2$, and clear relationships between DMS, SO$_2$, OH and H$_2$SO$_4$ (sulfuric acid) have been observed at a day length scale [*Davis et al.*, 1999]. Also, in this region it has been demonstrated that

aerosol nucleation and growth in the MBL is linked to the natural marine sulfur cycle [*Clarke et al.*, 1998].

[27] Over the North Pacific (region 5), strong mixed plumes of polluted (mainly nss-SO$_4$ and black carbon) and dust aerosols are emitted from Asia each spring and summer [*Husar et al.*, 1997; *Nagao et al.*, 1999; *Deuzé et al.*, 1999; *Prospero et al.*, 2002]. These are the dominant sources of CCN$_s$ over the region, in agreement with the low beta value obtained (13%). However, in terms of sulfur, the Asian anthropogenic source is estimated to provide only about 15–25% of the nss-SO$_4$ in the North Pacific [*Savoie et al.*, 1989]. For example, at Sheyma (50°N–170°E), although during spring nss-SO$_4$ is mainly from pollution, summertime nss-SO$_4$ is dominated by biogenic sources [*Savoie and Prospero*, 1989]. The subtropical North Pacific (region 6, $\beta = 30\%$) is less impacted by continental aerosols although they still dominate in the northern part of the

region close to the Asian continent [*Nagao et al.*, 1999] (see Figure 3). In this regard, over the subtropical northwestern Pacific a positive correlation was found between DMS_a and CCN in clean marine air and DMS was identified as a key factor in the production of nss-SO_4 and CCN [*Nagao et al.*, 1999]. Also, over more open ocean locations DMS can significantly contribute to the total nss-SO_4 burden. For example, at Midway Island ($28.22°N–177.3°W$) the annual contribution of DMS to the nss-SO_4 is estimated at $\approx 60\%$ [*Prospero et al.*, 2003].

[28] The Arctic (region 13, $\beta = 11\%$) is under the influence of SO_2 pollution from Europe and Asia [*Barrie et al.*, 1989]. The subtropical North Indian Ocean (region 10, $\beta = 12\%$) is characterized by very high levels of pollution aerosols during winter (NE monsoon) and by dust and SS during summer (SW monsoon) [*Johansen et al.*, 1999; *Tindale and Pease*, 1999; *Ramanathan et al.*, 2001; *Li and Ramanathan*, 2002]. Nevertheless, the fraction of nss-SO_4 derived from DMS is significant (from $\approx 20\%$ during the NE monsoon to $\approx 75\%$ during the SW monsoon [*Johansen et al.*, 1999]). During the NE monsoon, the contribution to the AOD of a 20% of natural nss-SO_4 is estimated to be very low (about a 5%) [*Satheesh et al.*, 2002]. Also, CCN properties over the Indian Ocean (North and South) differ depending on their origin: in polluted air masses, CCN particles have both a higher diameter and a higher percentage of refractory (nonvolatile) material than CCN in clean marine air [see *Ramanathan et al.*, 2001, Plate 7]. Finally, the lowest CCN_{bio} contribution occurs over the Mediterranean Sea (region 9, $\beta = 10\%$), a region mostly impacted by pollution from Europe and dust from Africa [*Husar et al.*, 1997; *Prospero et al.*, 2002]. In terms of sulfur, the maximum contribution of DMS to the nss-SO_4 is also low ($\approx 20–30\%$ in summer [*Kouvarakis and Mihalopoulos*, 2002; *Kubilay et al.*, 2002; *Kouvarakis et al.*, 2002]).

[29] Globally, the annual contribution of CCN_{bio} to the total CCN_s is estimated to be $\approx 30\%$. This value should be viewed as an upper end estimate since CCN_{bio} losses by rain washout were not taken into account. These results are in agreement with recent global models of the sulfur cycle that estimate the contribution of DMS to the global burden of nss-SO_4 to be $\approx 20–30\%$. Yet, similar to our findings, it can be more than an $80–90\%$ over the pollution-free SO in the austral summer [*Heintzenberg et al.*, 2000; *Gondwe et al.*, 2003, 2004; *Kloster et al.*, 2006]. All in all, this global estimate of the oceanic biogenic contribution to CCN has to taken with some caution due to the uncertainties going along with the approach used.

3.3. Uncertainty Analysis

[30] The estimates of the biogenic contribution to CCN_s carry an associated uncertainty that arises from the various uncertainties within the approach used: the satellite retrieval of CCN, sea surface DMS concentrations, DMS oxidation in the atmosphere. To address them all we have performed an uncertainty analysis (UA) by repeating the quantitative analyses under different conditions. The importance of the satellite retrieval of CCN_s has been evaluated by using an alternative set of CCN_s data (MODIS algorithm, which uses a different

method for CCN derivation) and comparing the results with those obtained with the modified version of the *Gassó and Hegg* [2003] algorithm used in the present study. The importance of uncertainties regarding the DMS oxidation has been addressed by increasing/decreasing the k_s constant of the oxidation efficiency γ parameter (see equation (3)) by 50%. The same approach has been used for the DMS_w concentrations (increase/decrease by 50%). Also, we have evaluated the confidence intervals of the current estimates of the biogenic contribution to the CCN_s by applying equation (2) using the upper and lower limits (95% confidence intervals) of the regression parameters obtained over the SO. That is, the upper end estimates of CCN_{bio} result from using the upper slope value with the lower intercept value; the lower end estimates of CCN_{bio} result from using the lower slope value with the higher intercept value. UA results are listed in auxiliary material Table S1[1]. Since the increase/decrease DMS_w did not produce any change, we have omitted it.

[31] Figure 8 displays the estimates of biogenic contribution to the CCN_s at each region of the global ocean for all these six UA scenarios. Maximum β estimates are given by the top of the color bars while minimum β estimates are given by the top of the black bars. At each of the 15 regions, we have then 3 columns (each one with a maximum and a minimum β value). The first column represents the results of the UA related to the CCN_s data set; the second one is the UA related to the DMS oxidation parameterization; and the third one is the UA related to the regression equation (confidence intervals of the regression parameters) used to estimate CCN_{bio}. In the first case, we obtain systematically higher biogenic contributions to CCN when using the MODIS CCN_s (dark gray bar) than with our CCN_s estimates (black bar; β values are from Figure 7). Similarly, an increase in the k_s constant produce higher β values in all the regions except the 13 (no change) and 15 (small decrease) (light gray bar versus black bar). The highest variability is obtained from the use of different equations (upper and lower confidence intervals) for CCN_{bio} estimates (third column; white bar versus black bar). The black stars denote the β values obtained by averaging the six scenarios; they are generally very close the value obtained for the standard case (the black bar in each first column, also Figure 7). Therefore, although the absolute values of the biogenic contribution estimates carry substantial uncertainty, the observed trends are robust enough. Only four regions show a dominant CCN_{bio} contribution to the total CCN_s numbers (more than $\approx 60\%$) and they are all located in the Southern Hemisphere (regions 4, 8, 12 and 14).

4. Conclusions

[32] On the basis of globally mapped seasonal correlations between climatological data, we have tested if oceanic DMS concentrations may be driven by the solar radiation dose in the upper mixed layer, if DMS emissions to the atmosphere are coupled to satellite-derived CCN concentrations, and if this biogenic contribution could be significant from a regional and global perspective. While seasonal

---

[1]Auxiliary materials are available at ftp://ftp.agu.org/apend/gb/2006gb002787.
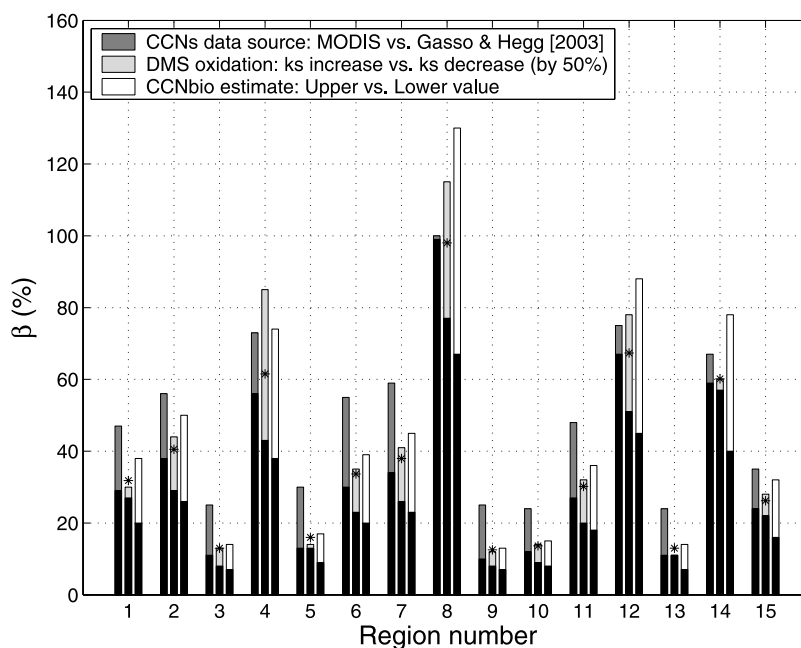
Figure 8. Uncertainty analysis of the estimated annual biogenic contribution to total CCN_s concentrations for 15 regions of the global ocean ($\beta = \frac{\sum CCN_{bio}}{\sum CCN_s} * 100$). For each region, the first column represents the uncertainty analysis related to the CCN_s data set (MODIS algorithm versus *Gassó and Hegg* [2003] algorithm); the second one is the uncertainty analysis related to the DMS oxidation parameterization (50% k_s increase versus 50% k_s decrease); and the third one is the uncertainty analysis related to the regression equation (confidence intervals of the parameters) use to estimate CCN_{bio}. Maximum β estimates are given by the top of the color bars while minimum β estimates are given by the top of the black bars.

correlations are never a proof of causality, they indicate the degree to which variables move in concert and can therefore be very useful to test hypotheses of mechanistic links between the variables and, if the correlations do not show the expected couplings, reject the hypotheses. Regarding the CLAW hypothesis, the obtained results do not contradict its main two postulates: (1) an increase (decrease) of solar irradiance can produce an increase (decrease) of seawater DMS (and then its emission to the atmosphere); (2) an increase (decrease) of DMS emissions can produce an increase (decrease) of CCN. They rather support them, although the observed couplings between DMS oxidation and CCN concentrations can only be attributable to a biogenic origin over clean regions of the Southern Hemisphere. However, our approach does not fully rule out that the observed correlation are due to an independent seasonal variation of the studied variables; seasonal couplings are "necessary but not sufficient" conditions to prove the CLAW hypothesis [*Bates et al.*, 1987]. Nevertheless, a sequence of observations point toward the existence of a negative feedback. Recent results have pointed out the possibility that DMS production has a protective function inside phytoplankton cells against high UV radiation [*Sunda et al.*, 2002], resulting in a constant leakage of this compound from the stressed cells into seawater. This, together with a complex web of biotic and abiotic processes, results in the accumulation of DMS in highly irradiated surface waters [*Simó and Pedrós-Alló*, 1999; *Toole and Siegel*,

2004; *Vallina and Simó*, 2007]. As solar radiation increases in summer, the subsequent increase of aqueous DMS would increase DMS emission to the atmosphere, its oxidation to nss-SO$_4$ aerosols, and CCN formation, which would reduce the level of solar radiation exposure of the surface ocean. The efficiency of this process would be enhanced if the main atmospheric DMS oxidant (the OH radical) increased also in summer, a period of maximum atmospheric vertical convection [*Barrie et al.*, 2001] that would facilitate the DMS-OH mixing and oxidation as well as a higher SO$_2$ to nss-SO$_4$ conversion efficiency [*Barrie et al.*, 2001]. All these steps are globally observed: DMS$_w$, DMS$_{flux}$, OH, nss-SO$_4$ and CCN, all increase in summer. These couplings are stronger at high latitudes, probably as a consequence of the higher seasonal amplitude of the solar irradiance. However, although the DMS (hemispheric) summer increase is widespread, only in the Southern Hemisphere the estimated biogenic production of CCN from DMS oxidation significantly contributes to the total CCN. In the Northern Hemisphere, which is under very high anthropogenic influence, the biogenic contribution to CCN is minor. Over equatorial to tropical regions, other sources also dominate CCN concentrations and variability owing to the low seasonality of solar irradiance and the heavy inputs of continental aerosols. From a global perspective, therefore, the contribution of biogenic CCN to the total CCN is rather moderate ($\approx$30%). However, over remote oceanic regions far from continental inputs (e.g., Southern Ocean, subtropical South

Pacific), CCN seem to be strongly influenced by CCN_{bio}. In this regard, it is in clean air over marine regions where changes in CCN concentrations may have greater impact on cloud albedo due to the lower droplet concentrations [*Platnick and Twomey*, 1994; *Van Dingenen et al.*, 1995; *Liss et al.*, 1997]. Over these regions a natural biogeochemical mechanism of climate regulation (as proposed by the CLAW hypothesis) could perfectly be operating, at least on seasonal timescales. It is then plausible that in pre-industrial periods a seasonal "solar radiation dose-DMS-CCN" link was globally important.

References

Albrecht, B. A. (1989), Aerosols, cloud microphysics, and fractional cloudiness, *Science, 245*(4923), 1227–1230.

Andreae, M. O., W. Elbert, Y. Cai, and T. W. Andreae (1999), Non-sea-salt sulfate, methanesulfonate, and nitrate aerosol concentrations and size distributions at Cape Grim, Tasmania, *J. Geophys. Res., 104*(D1), 21,695–21,706.

Andreae, M. O., T. W. Andreae, D. Meyerdierks, and C. Thiel (2003), Marine sulfur cycling and the atmospheric aerosol over the springtime North Atlantic, *Chemosphere, 52*, 1321–1343.

Arimoto, R. (2001), Eolian dust and climate: Relationships to sources, tropospheric chemistry, transport and deposition, *Earth Sci. Rev., 54*, 29–42.

Ayers, G. P., and R. W. Gillett (2000), DMS and its oxidation products in the remote marine atmosphere: Implications for climate and atmospheric chemistry, *J. Sea Res., 43*, 275–286.

Ayers, G. P., J. P. Ivey, and B. W. Forgan (1995), Dimethylsulfide in marine air at Cape Grim, 41°S, *J. Geophys. Res., 100*(D10), 21,013–21,021.

Ayers, G. P., J. M. Cainey, R. W. Gillett, and J. P. Ivey (1997), Atmospheric sulphur and cloud condensation nuclei air in marine air in the Southern Hemisphere, *Philos. Trans. R. Soc., Ser. B, 352*, 203–211.

Barrie, L. A., M. P. Olson, and K. K. Oikawa (1989), The flux of anthropogenic sulphur into the Arctic from mid-latitudes, *Atmos. Environ., 23*, 2502–2512.

Barrie, L. A., et al. (2001), A comparison of large-scale atmospheric sulphate aerosol models (COSAM): Overview and highlights, *Tellus, Ser. B, 53*, 615–645.

Bates, T. S., J. R. Charlson, and R. H. Gammon (1987), Evidence for the climatic role of marine biogenic sulfur, *Nature, 329*, 319–320.

Berresheim, H., M. O. Andreae, R. L. Iverson, and S. M. Li (1991), Seasonal variation of dimethylsulfide emissions and atmospheric sulfur and nitrogen species over the western north Atlantic Ocean, *Tellus, Ser. B, 43*, 353–372.

Brock, T. D. (1981), Calculating solar radiation for ecological studies, *Ecol. Modell., 14*, 1–19.

Charlson, R. J., J. E. Lovelock, M. O. Andreae, and S. G. Warren (1987), Oceanic phytoplankton, atmospheric sulfur, cloud albedo and climate, *Nature, 326*, 655–661.

Chin, M., D. L. Savoie, B. J. Huebert, A. R. Bandy, D. C. Thornton, T. S. Bates, P. K. Quinn, E. S. Saltzman, and W. J. De Bruyn (2000), Atmospheric sulfur cycle simulated in the global model GOCART: Comparison with field observations and regional budgets, *J. Geophys. Res., 105*(D20), 24,689–24,712.

Clarke, A. D., et al. (1998), Particle nucleation in the Tropical Boundary Layer and its couplings to marine sulfur sources, *Science, 282*, 89–92.

Cox, R. A. (1997), Atmospheric sulphur and climate: What have we learned?, *Philos. Trans. R. Soc., Ser. B, 352*, 251–254.

Cropp, R. A., A. J. Gabric, G. H. McTainsh, and R. D. Braddock (2005), Coupling between ocean biota and atmospheric aerosols: Dust, dimethylsulphide, or artifact?, *Global biogeochem. Cycles, 19*, GB4002, doi:10.1029/2004GB002436.

Curran, M. A. J., and G. B. Jones (1998), Spatial distribution of dimethylsulfide and dimethylsulfoniopropionate in the Australasian sector of the Southern Ocean, *J. Geophys. Res., 103*(D13), 16,677–16,689.

Davis, D., G. Chen, P. Kasibhatla, A. Jefferson, D. Tanner, F. Eisele, D. Lenschow, W. Neff, and H. Berresheim (1998), DMS oxidation in the Antarctic marine boundary layer: Comparison of model simulations and field observations of DMS, DMSO, $DMSO_2$, $H_2SO_2(g)$, MSA(g), and MSA(p), *J. Geophys. Res., 103*(D1), 1657–1678.

Davis, D., et al. (1999), Dimethylsulfide oxidation in the equatorial Pacific: Comparison of model simulations with field observations for DMS, SO_2, $H_2SO_2(g)$, MSA(g), MS, and NSS, *J. Geophys. Res., 104*(D5), 5765–5784.

Davison, B., C. N. Hewitt, C. D. O'Dowd, J. A. Lowe, and M. H. Smith (1996), Dimethyl sulfide, methane sulfonic acid and physicochemical aerosol properties in Atlantic air from the United Kingdom to Halley Bay, *J. Geophys. Res., 101*(D17), 22,855–22,867.

de Boyer Montégut, C., G. Madec, A. S. Fischer, A. Lazar, and D. Iudicone (2004), Mixed layer depth over the global ocean: An examination of profile data and a profile-based climatology, *J. Geophys. Res., 109*, C12003, doi:10.1029/2004JC002378.

De Bruyn, W. J., T. S. Bates, J. M. Cainey, and E. S. Saltzman (1998), Shipboard measurements of dimethylsulfide and SO_2 southwest of Tasmania during the First Aerosol Characterization Experiment (ACE1), *J. Geophys. Res., 103*(D13), 16,703–16,711.

Deuzé, J. L., M. Herman, P. Goloub, D. Tanré, and A. Marchand (1999), Characterization of aerosols over ocean from POLDER/ADEOS-1, *Geophys. Res. Lett., 26*(10), 1421–1424.

Duncan, B. N., R. V. Martin, A. C. Staudt, R. Yevich, and J. A. Logan (2003), Interannual and seasonal variability of biomass burning emissions constrained by satellite observations, *J. Geophys. Res., 108*(D2), 4100, doi:10.1029/2002JD002378.

Fiore, A. M., D. J. Jacob, H. Liu, R. M. Yantosca, T. D. Fairlie, and Q. B. Li (2003), Variability in surface ozone background over the United States: Implications for air quality policy, *J. Geophys. Res., 108*(D24), 4787, doi:10.1029/2003JD003855.

Fitzgerald, J. W. (1991), Marine aerosols: A review, *Atmos. Environ., Part A, 25*, 533–545.

Gassó, S., and D. A. Hegg (2003), On the retrieval of columnar aerosol mass and CCN concentration by MODIS, *J. Geophys. Res., 108*(D1), 4010, doi:10.1029/2002JD002382.

Ginoux, P., M. Chin, I. Tegen, J. M. Prospero, B. Holben, O. Dubovik, and S.-J. Lin (2001), Sources and distributions of dust aerosols simulated with the GOCART model, *J. Geophys. Res., 106*(D17), 20,255–20,273.

Goloub, P., and O. Arino (2000), Verification of the consistency of POLDER Aerosol Index over land with ATSR-2/ERS-2 fire product, *Geophys. Res. Lett., 27*(6), 899–902.

Gondwe, M., M. Krol, W. Gieskes, W. Klaassen, and H. de Baar (2003), The contribution of ocean-leaving DMS to the global atmospheric burdens of DMS, MSA, SO_2, and NSS $SO_4^=$, *Global Biogeochem. Cycles, 17*(2), 1056, doi:10.1029/2002GB001937.

Gondwe, M., M. Krol, W. Klaassen, W. Gieskes, and H. de Baar (2004), Comparison of modeled versus measured MSA:nss-$SO_4^=$ ratios: A global analysis, *Global Biogeochem. Cycles, 18*, GB2006, doi:10.1029/2003GB002144.

Heintzenberg, J., D. C. Covert, and R. Van Dingenen (2000), Size distribution and chemical composition of marine aerosols: A compilation and review, *Tellus, Ser. B, 52*, 1104–1122.

Husar, R. B., J. M. Prospero, and L. L. Stowe (1997), Characterization of tropospheric aerosols over the oceans with the NOAA Advanced Very High Resolution Radiometer optical thickness operational product, *J. Geophys. Res., 102*(D14), 16,889–16,909.

Ichoku, C., Y. J. Kaufman, L. A. Remer, and R. Levy (2004), Global aerosol remote sensing from MODIS, *Adv. Space Res., 34*, 820–827.

Johansen, A. M., R. L. Siefert, and M. R. Hoffmann (1999), Chemical characterization of ambient aerosol collected during the southwest monsoon and intermonsoon seasons over the Arabian Sea: Anions and cations, *J. Geophys. Res., 104*(D21), 26,325–26,347.

Jourdain, B., and M. Legrand (2001), Seasonal variations of atmospheric dimethylsulfide, dimethylsulfoxide, sulfur dioxide, methanesulfonate, and non-sea-salt sulfate aerosols at Dumont d'Urville (coastal Antarctica) (December 1998 to July 1999), *J. Geophys. Res., 106*(D13), 14,391–14,408.

Kaufman, Y. J., D. Tanré, and O. Boucher (2002), A satellite view of aerosols in the climate system, *Nature, 419*, 215–223.

Kettle, A. J., and M. O. Andreae (2000), Flux of dimethylsulfide from the oceans: A comparison of updated data set and flux models, *J. Geophys. Res.*, *105*(D22), 26,793–26,808.

Kieber, D. J., J. Jiao, R. P. Kiene, and T. S. Bates (1996), Impact of dimethylsulfide photochemistry on methyl sulfur cycling in the equatorial Pacific Ocean, *J. Geophys. Res.*, *101*(C2), 3715–3722.

Kiehl, J. T., and E. Trenberth (1997), Earth's annual global mean energy budget, *Bull. Am. Meteorol. Soc.*, *78*(2), 197–208.

Kistler, R., et al. (2001), The NCEP-NCAR 50-Year Reanalysis: Monthly means CD-ROM and documentation, *Bull. Am. Meteorol. Soc.*, *82*(2), 247–267.

Kloster, S., J. Feichter, E. Maier-Reimer, K. D. Six, and P. Stier (2006), DMS cycle in the marine ocean-atmosphere system—A global model study, *Biogeosciences*, *3*, 29–51.

Kouvarakis, G., and N. Mihalopoulos (2002), Seasonal variation of dimethylsulfide in the gas phase and of methanesulfonate and non-sea-salt sulfate in the aerosol phase in the Mediterranean atmosphere, *Atmos. Environ.*, *36*, 929–938.

Kouvarakis, G., H. Bardouki, and N. Mihalopoulos (2002), Sulfur budget above the eastern Mediterranean: relative contribution of anthropogenic and biogenic sources, *Tellus, Ser. B*, *54*, 201–212.

Kubilay, N., M. Koçak, T. Çokacar, T. Oguz, G. Kouvarakis, and N. Mihalopoulos (2002), Influence of Black Sea and local biogenic activity on the seasonal variation of aerosol sulfur species in the eastern Mediterranean atmosphere, *Global Biogeochem. Cycles*, *16*(4), 1079, doi:10.1029/2002GB001880.

Lee, Z. P., K. P. Du, R. Arnone, S. C. Liew, and B. Penta (2005), Penetration of solar radiation in the upper ocean: A numerical model for oceanic and coastal waters, *J. Geophys. Res.*, *110*, C09019, doi:10.1029/2004JC002780.

Lefohn, A. S., J. D. Husar, and R. B. Husar (1999), Estimating historical anthropogenic global sulfur emission patterns for the period 1850–1990, *Atmos. Environ.*, *33*, 3435–3444.

Li, F., and V. Ramanathan (2002), Winter to summer monsoon variation of aerosol optical depth over the tropical Indian Ocean, *J. Geophys. Res.*, *107*(D16), 4284, doi:10.1029/2001JD000949.

Li-Jones, X., and J. M. Prospero (1998), Variations in the size distribution of non-sea-salt sulfate aerosol in the marine boundary layer at Barbados: Impact of African dust, *J. Geophys. Res.*, *103*(D13), 16,073–16,084.

Liss, P. S., A. D. Hatton, G. Malin, P. D. Nightingale, and S. M. Turner (1997), Marine sulphur emissions, *Philos. Trans. R. Soc., Ser. B*, *352*, 159–169.

Martin, J. H., et al. (1994), Testing the iron hypothesis in ecosystems of the equatorial Pacific Ocean, *Nature*, *371*, 123–129.

Miller, A. J., et al. (2003), Potential feedbacks between Pacific Ocean ecosystems and interdecadal climate variations, *Bull. Am. Meteorol. Soc.*, *84*, 617–633.

Minikin, A., M. Legrand, J. Hall, D. Wagenbach, C. Kleefeld, E. Wolff, E. C. Pasteur, and F. Ducroz (1998), Sulfur-containing species (sulfate and methanesulfonate) in coastal Antarctic aerosol and precipitation, *J. Geophys. Res.*, *103*(D9), 10,975–10,990.

Murphy, D. M., J. R. Anderson, P. K. Quinn, L. M. McInnes, F. J. Brechtel, S. M. Kreidenweis, A. M. Middlebrook, M. Pósfai, D. S. Thomson, and P. R. Buseck (1998), Influence of sea-salt on aerosol radiative properties in the Southern Ocean marine boundary layer, *Nature*, *392*, 62–65.

Nagao, I., K. Matsumoto, and H. Tanaka (1999), Characteristics of dimethylsulfide, ozone, aerosols, and cloud condensation nuclei in air masses over the northwestern Pacific Ocean, *J. Geophys. Res.*, *104*(D9), 11,675–11,693.

Nightingale, P. D., P. S. Liss, and P. Schlosser (2000), Measurements of air-sea gas transfer during an open ocean algal bloom, *Geophys. Res. Lett.*, *27*, 2117–2120.

Perry, K. D., T. A. Cahill, R. A. Eldred, D. D. Dutcher, and T. E. Gill (1997), Long-range transport of North African dust to the eastern United States, *J. Geophys. Res.*, *102*(D10), 11,225–11,238.

Platnick, S., and S. Twomey (1994), Determining the susceptibility of cloud albedo to changes in droplet concentration with the advanced very high resolution radiometer, *J. Appl. Meteorol.*, *33*(3), 334–347.

Prospero, J. M. (1996), The atmospheric transport of particles to the ocean, in *Particle Flux in the Ocean*, edited by V. Ittekkot et al., pp. 133–151, John Wiley, Hoboken, N. J.

Prospero, J. M., P. Ginoux, O. Torres, S. E. Nicholson, and T. E. Gill (2002), Environmental characterization of global sources of atmospheric soil dust identified with the Nimbus 7 Total Ozone Mapping Spectrometer (TOMS) absorbing aerosol product, *Rev. Geophys.*, *40*(1), 1002, doi:10.1029/2000RG000095.

Prospero, J. M., D. L. Savoie, and R. Arimoto (2003), Long-term record of nss-sulfate and nitrate in aerosols on Midway Island, 1981–2000: Evidence of increased (now decreasing?) anthropogenic emissions from Asia, *J. Geophys. Res.*, *108*(D1), 4019, doi:10.1029/2001JD001524.

Quinn, P. K., D. J. Coffman, V. N. Kapustin, and T. S. Bates (1998), Aerosol optical properties in the marine boundary layer during the First Aerosol Characterization Experiment (ACE-1) and the underlying chemical and physical aerosol properties, *J. Geophys. Res.*, *103*(D13), 16,547–16,563.

Ramanathan, V., et al. (2001), Indian Ocean Experiment: An integrated analysis of the climate forcing and effects of the great Indo-Asian haze, *J. Geophys. Res.*, *106*(D22), 28,371–28,398.

Rasch, P. J., M. C. Barth, J. T. Kiehl, S. E. Schwartz, and C. M. Benkovitz (2000), A description of the global sulfur cycle and its controlling processes in the National Center for Atmospheric Research Community Climate Model, version 3, *J. Geophys. Res.*, *105*(D1), 1367–1385.

Remer, L. A., et al. (2005), The MODIS aerosol algorithm, products and validation, *J. Atmos. Sci.*, *62*, 947–973.

Reynolds, R. W., and T. M. Smith (1995), A high-resolution global sea surface temperature climatology, *J. Clim.*, *8*, 1571–1583.

Ross, K. E., S. J. Piketh, R. T. Bruintjes, R. P. Burger, R. J. Swap, and H. J. Annegarn (2003), Spatial and seasonal variations in CCN distribution and the aerosol-CCN relationship over southern Africa, *J. Geophys. Res.*, *108*(D13), 8481, doi:10.1029/2002JD002384.

Rotstayn, L. D., and U. Lohmann (2002), Simulation of the tropospheric sulfur cycle in a global model with a physically based cloud scheme, *J. Geophys. Res.*, *107*(D21), 4592, doi:10.1029/2002JD002128.

Sarmiento, J. L., et al. (2004), Response of ocean ecosystems to climate warming, *Global Biogeochem. Cycles*, *18*, GB3003, doi:10.1029/2003GB002134.

Satheesh, S. K., V. Ramanathan, X. Li-Jones, J. M. Lobert, I. A. Podgorny, J. M. Prospero, B. N. Holben, and N. G. Loeb (1999), A model for the natural and anthropogenic aerosols over the tropical Indian Ocean derived from Indian Ocean Experiment data, *J. Geophys. Res.*, *104*(D22), 27,421–27,440.

Satheesh, S. K., V. Ramanathan, B. N. Holben, K. K. Moorthy, N. G. Loeb, H. Maring, J. M. Prospero, and D. Savoie (2002), Chemical, microphysical, and radiative effects of Indian Ocean aerosols, *J. Geophys. Res.*, *107*(D23), 4725, doi:10.1029/2002JD002463.

Savoie, D. L., and J. M. Prospero (1989), Comparison of oceanic and continental sources of non-sea-salt sulphate over the Pacific Ocean, *Nature*, *339*, 685–687.

Savoie, D. L., J. M. Prospero, and E. S. Saltzman (1989), Nitrate, non-seasalt sulfate and methanesulfonate over the Pacific Ocean, in *Chemical Oceanography*, vol. 10, edited by J. Riley and R. Chester, pp. 220–250, Elsevier, New York.

Savoie, D. L., J. M. Prospero, R. J. Larsen, and E. S. Saltzman (1992), Nitrogen and sulfur species in aerosols at Mawson, Antarctica, and their relationship to natural radionuclides, *J. Atmos. Chem.*, *14*, 181–204.

Savoie, D. L., J. M. Prospero, R. Arimoto, and R. A. Duce (1994), Non-sea-salt sulfate and methanesulfonate at American Samoa, *J. Geophys. Res.*, *99*(D2), 3587–3596.

Savoie, D. L., R. Arimoto, W. C. Keene, J. M. Prospero, R. A. Duce, and J. N. Galloway (2002), Marine biogenic and anthropogenic contributions to non-sea-salt sulfate in the marine boundary layer over the North Atlantic Ocean, *J. Geophys. Res.*, *107*(D18), 4356, doi:10.1029/2001JD000970.

Sciare, J., E. Baboukas, R. Hancy, N. Mihalopoulos, and B. C. Nguyen (1998), Seasonal variation of dimethylsulfoxide in rainwater at Amsterdam Island in the Southern Indian Ocean: Implications on the biogenic sulfur cycle, *J. Atmos. Chem.*, *30*, 229–240.

Sciare, J., N. Mihalopoulos, and F. J. Dentener (2000), Interannual variability of atmospheric dimethylsulfide in the southern Indian Ocean, *J. Geophys. Res.*, *105*(D21), 26,369–26,377.

Shon, Z.-H., et al. (2001), Evaluation of the DMS flux and its conversion to SO_2 over the Southern Ocean, *Atmos. Environ.*, *35*, 159–172.

Simó, R. (2001), Production of atmospheric sulfur by oceanic plankton: Biogeochemical, ecological and evolutionary links, *Trends Ecol. Evol.*, *16*(6), 287–294.

Simó, R., and J. Dachs (2002), Global ocean emission of dimethylsulfide predicted from biogeophysical data, *Global biogeochem. Cycles*, *16*(4), 1018, doi:10.1029/2001GB001829.

Simó, R., and C. Pedros-Allió (1999), Role of vertical mixing in controlling the oceanic production of dimethyl sulphide, *Nature*, *402*, 396–399.

Smith, R. C., and K. S. Baker (1979), Penetration of UV-B and biologically effective dose-rates in natural waters, *Photochem. Photobiol.*, *29*, 311–323.

Smith, S. J., H. Pitcher, and T. M. L. Wigley (2001), Global and regional anthropogenic sulfur dioxide emissions, *Global Planet. Change*, *29*, 99–119.

Sunda, W., D. J. Kieber, R. P. Kiene, and S. Huntsman (2002), An antioxidant function for DMSP and DMS in marine algae, *Nature*, *418*, 317–320.

Swap, R., M. Garstang, and S. Greco (1992), Saharan dust in the Amazon Basin, *Tellus, Ser. B*, *44*, 133–149.

Tanré, D., L. A. Remer, Y. J. Kaufman, S. Mattoo, P. V. Hobbs, J. M. Livingston, P. B. Russell, and A. Smirnov (1999), Retrieval of aerosol optical thickness and size distribution over ocean from the MODIS airborne simulator during TARFOX, *J. Geophys. Res.*, *104*(D2), 2261–2278.

Tanré, D., F. M. Bréon, J. L. Deuzé, M. Herman, P. Goloub, F. Nadal, and A. Marchand (2001), Global observations of anthropogenic aerosols from satellite, *Geophys. Res. Lett.*, *28*(24), 4555–4558.

Tindale, N. W., and P. P. Pease (1999), Aerosols over the Arabian Sea: Atmospheric transport pathways and concentrations of dust and sea salt, *Deep Sea Res., Part II*, *46*, 1577–1595.

Toole, D. A., and D. A. Siegel (2004), Light-driven cycling of dimethylsulfide (DMS) in the Sargasso Sea: Closing the loop, *Geophys. Res. Lett.*, L09308, doi:10.1029/2004GL019581.

Twomey, S. (1974), Pollution and planetary albedo, *Atmos. Environ.*, *8*, 1251–1256.

Vallina, S. M., and R. Simó (2007), Strong relationship between DMS and the solar radiation dose over the global surface ocean, *Science*, *315*, 506–509.

Vallina, S. M., R. Simó, and S. Gassó (2006), What controls CCN seasonality in the Southern Ocean? A statistical analysis based on satellite-derived chlorophyll and CCN and model-estimated OH radical and rainfall, *Global Biogeochem. Cycles*, *20*, GB1014, doi:10.1029/2005GB002597.

Van Dingenen, R., F. Raes, and N. R. Jensen (1995), Evidence for anthropogenic impact on number concentration and sulfate content of cloud-processed aerosol particles over the North Atlantic, *J. Geophys. Res.*, *100*(D10), 21,057–21,067.

Wilson, C., and V. J. Coles (2005), Global climatological relationships between satellite biological and physical observations and upper ocean properties, *J. Geophys. Res.*, *110*, C10001, doi:10.1029/2004JC002724.

Wylie, D. J., and J. de Mora (1996), Atmospheric dimethylsulfide and sulfur species in aerosol and rainwater at a coastal site in New Zealand, *J. Geophys. Res.*, *101*(D15), 21,041–21,049.

Yoon, Y. J., and P. Brimblecombe (2002), Modelling the contribution of sea salt and dimethylsulfide derived aerosol to marine CCN, *Atmos. Chem. Phys.*, *2*, 17–30.

———————————

J. Dachs and E. Jurado, Department of Environmental Chemistry, IIQAB-CSIC, Jordi Girona 18-26, E-08034 Barcelona, Spain. (jdmqam@cid.csic.es; jurado.elena@gmail.com)

C. de Boyer-Montégut, Yokohama Institute for Earth Sciences, JAMSTEC-FRCGC, 3173-25 Showa-machi, Kanazawa-ku, Yokohama, Kanagawa 236-0001, Japan. (clement@jamstec.go.jp)

E. del Río and R. Simó, Institut de Ciències del Mar de Barcelona (ICM–CSIC), Passeig Marítim de la Barceloneta, 37-49, E-08003 Barcelona, Spain. (edelrio@cmima.csic.es; rsimo@icm.csic.es)

S. Gassó, Goddard Earth Science and Technology Center, University of Maryland, NASA/GSFC, Greenbelt, MD 20771, USA. (santiago@climate.gsfc.nasa.gov)

S. M. Vallina, Laboratory for Global Marine and Atmospheric Chemistry, School of Environmental Sciences, University of East Anglia, Norwich NR4 7TJ, UK. (sergio.vallina@uea.ac.uk)

Table S1. Uncertainty analysis of the estimated annual biogenic contribution to total CCN_s concentrations for 15 regions of the global ocean ($\beta = \frac{\sum CCN_{bio}}{\sum CCN_s} * 100$) and of the correlation coefficient (ρ) between CCN_{bio} and total $CCN_s{}^a$

	CCN$_{bio}$ vs. CCN$_s$ for:									
Station	Lower estimates		Upper estimates		k_s -50%		k_s +50%		MODIS CCN$_s$	
	ρ	β	ρ	β	ρ	β	ρ	β	ρ	β
1	0.92	20%	0.92	38%	0.92	27%	0.89	30%	0.95	47%
2	0.72	26%	0.72	50%	0.72	29%	0.72	44%	0.77	56%
3	-0.22	7%	-0.22	14%	-0.22	8%	-0.22	13%	-0.64	25%
4	-0.32	38%	-0.32	74%	-0.38	43%	-0.31	85%	0.02	73%
5	0.91	9%	0.91	17%	0.84	13%	0.91	14%	0.92	30%
6	0.58	20%	0.58	39%	0.6	23%	0.58	35%	0.5	55%
7	-0.17	23%	-0.17	45%	-0.23	26%	-0.13	41%	0.31	59%
8	0.68	67%	0.68	130%	0.59	77%	0.68	115%	0.69	100%
9	0.64	7%	0.64	13%	0.55	8%	0.68	12%	0.62	25%
10	-0.17	8%	-0.17	15%	-0.17	9%	-0.17	14%	0.71	24%
11	0.17	18%	0.17	36%	0.17	20%	0.22	32%	0.9	48%
12	0.31	45%	0.31	88%	0.24	51%	0.35	78%	0.12	75%
13	0.98	7%	0.98	14%	0.97	11%	0.98	11%	1.0	24%
14	0.9	40%	0.9	78%	0.88	57%	0.92	60%	0.94	67%
15	0.95	16%	0.95	32%	0.89	28%	0.95	22%	0.96	35%

^{a} See text for further details.

Paper 2006GB002787 Auxiliary Material